



The Study of Estimating Peanut Yield Based on Drone Multispectral Remote Sensing

Xinyu Zou

Changchun University of Science and Technology, Changchun, Jilin, China

Abstract: This study utilized drone aerial operations to capture multispectral remote sensing images of peanut fields during three flights on July 10, August 22, and September 20, 2024. Band calculations were performed using vegetation index formulas to derive vegetation index data. In the study area, yield data was collected based on sampling regions. Using vegetation index data as the independent variable and actual yield as the dependent variable, linear regression, curve statistics, multiple linear regression, and machine learning methods were employed to construct and validate yield estimation models. The performance of each model on the validation set was compared, leading to the identification of the optimal yield estimation model. This research provides a relatively precise approach for estimating peanut yield based on drone multispectral remote sensing, achieving real-time and rapid monitoring of peanut yield in the study area. It lays a solid foundation for establishing an economical, applicable, and efficient peanut yield estimation system and offers a reference for decision-making in precision agriculture.

Keywords: drone remote sensing; multispectral; vegetation index; peanuts; yield estimation; machine learning.

1. Introduction

China is the world's largest producer and consumer of peanuts. Peanuts are an important livelihood crop and a key industry for promoting rural economies; they not only serve as a vital agricultural product for safeguarding livelihoods but also act as a significant pillar for driving rural economic development. Satellite remote sensing methods for yield estimation are suitable for large-scale crop yield assessments; however, for smaller areas, the longer repetitive cycles, lower temporal and spatial resolutions, and susceptibility to atmospheric conditions limit their ability to obtain accurate ground information in a timely manner, resulting in limited effectiveness for crop yield forecasting. The rapid development of drone remote sensing technology effectively addresses these shortcomings of satellite remote sensing. Drone remote sensing for yield estimation mainly draws on satellite remote sensing methods, boasting advantages such as lower costs, lower flying altitudes, higher spatial resolution, real-time capabilities, and minimal atmospheric interference, thus providing new technological means for crop yield estimation and land cover classification on a small scale, which is significantly important for the monitoring and development of agricultural crops.

Mengsen Luo et al. have overcome the limitations of traditional linear models and began to use artificial neural networks as a new algorithm to establish non-linear yield prediction models, discovering that the accuracy of neural network models is higher than that of linear models. After incorporating the Normalized Difference Water Index (NDWI) into their models, Bolton et al. found that the accuracy of the yield estimation models improved, indicating that the integration of different spectral parameters can indeed enhance the predictive stability of the models. N.T. Son and colleagues constructed a joint model of Enhanced Vegetation Index (EVI) and Leaf Area Index (LAI) based on MODIS satellite data, finding that the model's accuracy improved compared to single indicator models, while also demonstrating adaptability to other regions. Wen-Ting Han et al. focused their research on Inner Mongolia Autonomous Region, utilizing a multispectral camera mounted on a drone to perform multi-temporal remote sensing monitoring of summer corn under different moisture treatments, and employed the least squares method to construct a remote sensing yield estimation model based on multiple vegetation indices and multi-temporal data. Their findings indicated that the yield estimation model using GNDVI across multiple growth stages had the highest accuracy, with an R^2 of 0.89. Fei and colleagues employed a method combining multi-sensor data fusion and machine learning for wheat yield prediction. They utilized various regression models, including Support Vector Machine (SVM), Deep Neural Network (DNN), and Random Forest (RF). When data from multiple sensors, including RGB, multispectral, and thermal spectral data, were merged and integrated learning was achieved, the highest R^2 value reached 0.89.

2. Materials and Methods

2.1 Overview of the Study Area

The study area is located in Yanjin County, Xinxiang City, Henan Province, with geographic coordinates of 35°29'N latitude and 114°30'E longitude, as shown in Figure 1. This area belongs to a warm temperate continental monsoon climate, characterized by distinct seasons with cold winters, hot summers, cool autumns, and early springs. The average annual temperature is approximately 14°C, with an annual precipitation of about 573.4 millimeters. The average temperature in July is around 27°C, while in January, it is approximately 0°C. The frost-free period lasts about 220 days, with an annual sunshine duration of around 2400 hours. The area of the study site is approximately 2 hectares, and the soil type is sandy soil. The peanut variety grown in the study area is “Peanut 9719,” with a planting date of June 1, 2024, and a harvesting date of October 1, 2024, resulting in a total growth duration of 123 days.

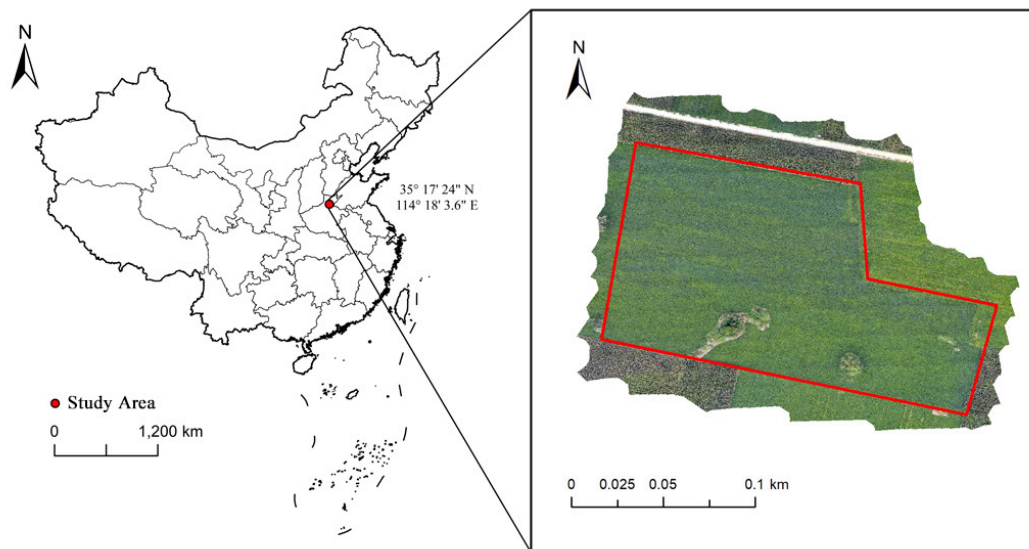


Figure 1. Overview of the Study Area

2.2 Data Acquisition

The unmanned aerial vehicle (UAV) used in this study is the DJI Phantom 4 Multispectral version, which is equipped with a visible light color sensor and five multispectral monochrome sensors. The camera model utilized is the P4 Multispectral Camera. Before the flight, it is essential to ensure clear weather and that wind speeds do not exceed level 4. The flight time is scheduled between 12:00 and 14:00, with specific flight parameter settings shown in Table 1.

Table 1. UAV Flight Parameters

Parameter Name	Parameter Value
Flight Height	30m
Flight Speed	2.1m/s
Ground Resolution	1.6cm/px
Forward Overlap Ratio	80%
Side Overlap Ratio	70%
Total Flight Line Length	3217m
Main Flight Line Angle	103°

Combining the growth cycle of Peanut 9719, the remote sensing data collection was conducted on July 10, 2024 (36 days after planting), August 22, 2024 (69 days after planting), and September 20, 2024 (108 days after planting). The method for harvesting the peanuts involved manual collection. During the harvesting process, peanuts were collected and sun-dried at each sampling point within their respective areas, ensuring no interference between them. In this study, remote sensing images were collected using DJI drones, and the locations of the peanut field sampling points were pre-determined

in ArcGIS software, along with the corresponding boundaries for each sampling area, to facilitate sampling on the designated harvesting days.

As shown in Figure 2, there are a total of 93 sampling points in the study area. Using ArcGIS software, the latitude and longitude information for each sampling point was obtained. Based on this information, the specific locations were identified prior to the harvesting day, and the corresponding sampling points and areas were marked. The data from the 93 sampling points collected in this study were divided into 80 data points for the training set and 13 data points for the validation set. When constructing the yield estimation model, only the training set data was used, while the validation set data was not involved in the fitting and machine learning process, serving solely for the validation of the yield estimation model.

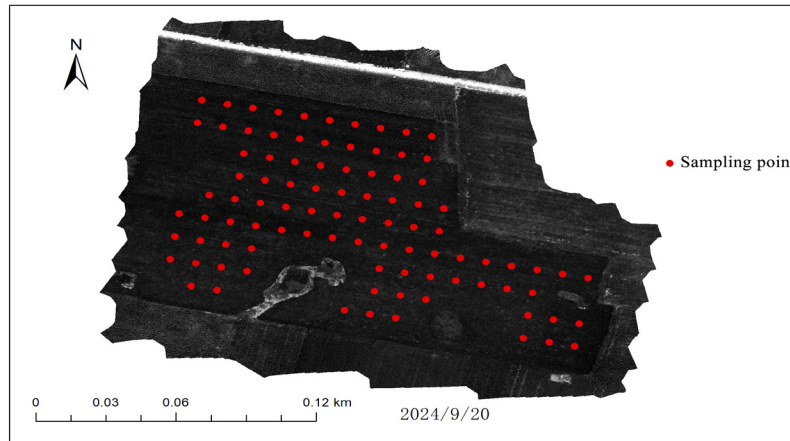


Figure 2. Sampling Point Information

2.3 Selection of Vegetation Indices

Vegetation indices are numerical values calculated using the reflectance from different spectral bands. In this study, four types of vegetation indices were selected: the Normalized Difference Vegetation Index (NDVI), the Green Normalized Difference Vegetation Index (GNDVI), the Normalized Difference Red Edge Index (NDRE), and the Land Cover Vegetation Index (LCI). The calculation formulas for each vegetation index are provided in Table 2.

Table 2. Vegetation Index Calculation Formulas

Vegetation Index	Calculation Formula
NDVI	$NDVI = \frac{NIR - R}{NIR + R}$
GNDVI	$GNDVI = \frac{NIR - G}{NIR + G}$
NDRE	$NDRE = \frac{NIR - RE}{NIR + RE}$
LCI	$LCI = \frac{NIR - RE}{NIR + R}$

Note: In the formulas, R, G, RE, and NIR represent the reflectance of the red, green, red edge, and near-infrared spectral bands, respectively.

2.4 Research Methodology

This study aims to explore the relationship between vegetation indices and crop yield, and to establish corresponding predictive models. Various vegetation index values were calculated through spectral band operations, including the Normalized Difference Vegetation Index (NDVI), the Green Normalized Difference Vegetation Index (GNDVI), the Normalized Difference Red Edge Index (NDRE), and the Land Cover Vegetation Index (LCI). Linear regression, curve statistical analysis, multiple linear regression, and machine learning methods were employed to analyze the correlation between vegetation indices and crop yield and to establish fitting models. Subsequently, the test set data was used to validate and evaluate the models. Ultimately, based on the results of model validation, the optimal model was compared and selected,

while an ensemble model was constructed using a weighted approach to enhance the stability of crop yield predictions.

3. Results and Analysis

3.1 Correlation Analysis of Vegetation Indices and Yield

Correlation analyses were conducted between the four vegetation indices and peanut yield during various growth stages, and the results are presented in Table 3.

	Vegetation Index	Correlation Coefficient (r)
Seedling Stage	NDVI	0.152
	GNDVI	0.201
	NDRE	0.150
	LCI	0.134
Pod-Setting Stage	NDVI	0.581
	GNDVI	0.541
	NDRE	0.566
	LCI	0.495
Maturation Stage	NDVI	0.780
	GNDVI	0.718
	NDRE	0.745
	LCI	0.750

According to Table 3, there are significant differences in the correlation coefficients between vegetation indices and peanut yield at different growth stages. In the early stages of peanut planting, the correlation coefficients of NDVI, GNDVI, NDRE, and LCI with peanut yield are 0.152, 0.201, 0.150, and 0.134, respectively, indicating a relatively low correlation. By the pod-setting stage, the correlation between the vegetation indices and peanut yield significantly increases, with the coefficients for NDVI, GNDVI, NDRE, and LCI reaching 0.581, 0.541, 0.566, and 0.495, respectively. During the maturity stage, the correlation further strengthens, with the coefficients for NDVI, GNDVI, NDRE, and LCI reaching 0.780, 0.718, 0.745, and 0.750, respectively, indicating a strong positive correlation. This suggests that as the growth stages of peanuts advance, the correlation between vegetation indices and peanut yield gradually strengthens.

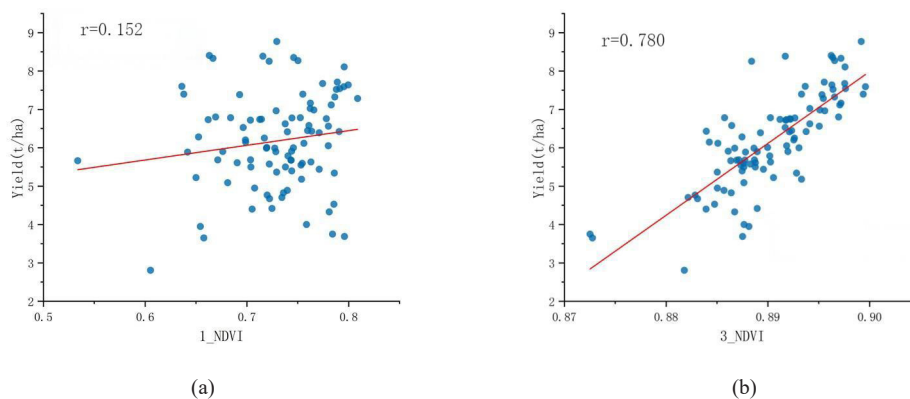


Figure 3. Correlation between Vegetation Indices and Yield: (a) NDVI during the Seedling Stage; (b) NDVI during the Maturity Stage.

3.2 Construction of Single Vegetation Index Yield Estimation Models

3.2.1 Linear Regression

As indicated by the previous correlation analysis between vegetation indices and yield, the vegetation indices during the maturity stage have the highest correlation with yield. Consequently, yield estimation models were established for the four vegetation indices during this stage, with the results presented in Table 4.

Table 4. Linear Fitting Model for Peanut Yield Estimation

Vegetation Index	Yield Estimation Model	R2	RMSE
NDVI	$y=194.61x-167.10$	0.581	0.815
GNDVI	$y=78.087x-53.330$	0.454	0.930
NDRE	$y=53.780x-9.690$	0.507	0.884
LCI	$y=46.812x-13.960$	0.516	0.876

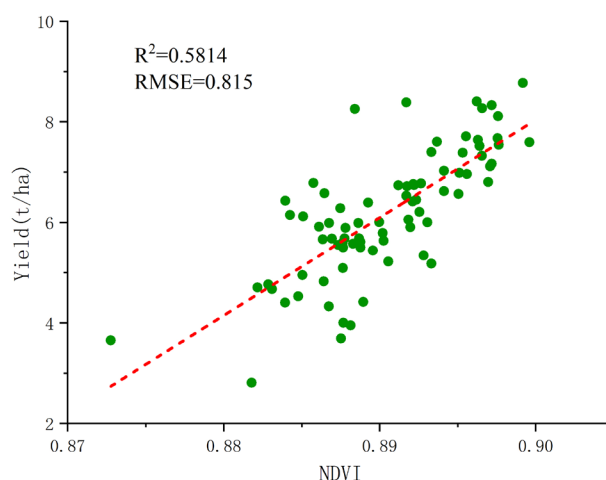


Figure 4. Scatter Plot of Yield-NDVI Estimation Model

From Table 4, it can be seen that there are significant differences in the estimation accuracy of yield models based on different vegetation indices during the peanut maturity stage. The coefficients of determination (R^2) for several models range from 0.454 to 0.581. Except for the GNDVI model, which has an R^2 below 0.5, all other vegetation index models are above 0.5. Among them, the remote sensing yield estimation model constructed with the NDVI index has the highest R^2 of 0.581 and the lowest RMSE of 0.815. In summary, the yield-NDVI model is the optimal single vegetation index linear yield estimation model, with the fitted estimation model equation given as $y = 194.61x - 167.10$.

3.2.2 Curve Fitting

Power function, quadratic polynomial, and logarithmic function curve statistical yield estimation models were established for the vegetation indices and actual peanut yield during the maturity stage (Table 5).

Table 5. Curve Fitting Model for Peanut Yield Estimation

Function	Vegetation Index	Yield Estimation Model	R2	RMSE
Power Function	NDVI	$y= 180.781x^{29.1999}$	0.593	0.803
	GNDVI	$y= 88.415x^{9.8254}$	0.459	0.927
	NDRE	$y= 137.66x^{2.5479}$	0.508	0.884
	LCI	$y= 93.451x^{3.2289}$	0.516	0.876
Quadratic Polynomial	NDVI	$y= 2746.5-6357.6x+ 3683.6x^2$	0.593	0.808
	GNDVI	$y= 337.9-950.1x+675.3x^2$	0.462	0.932
	NDRE	$y= -1.63-0.61x+91.43x^2$	0.515	0.889
	LCI	$y= -0.22-18.83x+75.83x^2$	0.520	0.881
Logarithmic Function	NDVI	$y= -20.32*\ln(-6.36*\ln(x))$	0.586	0.810
	GNDVI	$y= -16.22*\ln(-2.52*\ln(x))$	0.456	0.929
	NDRE	$y=-19.38*\ln(-0.595*\ln(x))n(x)$	0.507	0.884
	LCI	$y=-16.96*\ln(-0.824*\ln(x))$	0.517	0.876

Note: The R^2 values for the power function yield-NDVI and the quadratic polynomial yield-NDVI are both 0.593 when rounded to three decimal places. However, when rounded to five decimal places, the R^2 for the power function yield-NDVI is 0.59305, and for the quadratic polynomial yield-NDVI, it is 0.59344, slightly higher than that of the power function yield-NDVI.

From Table 5, it can be seen that all three curve statistical yield estimation models show varying degrees of improvement compared to linear fitting. Among them, the polynomial curve statistical yield estimation models have R² values higher than those of other curve statistical models. In the polynomial curve statistical yield estimation models, the yield-NDVI has the highest R², reaching 0.593, with an RMSE of 0.808. Furthermore, in the other curve statistical yield estimation models, the yield estimation model constructed with the NDVI vegetation index and actual yield has a coefficient of determination (R²) higher than those of the estimation models based on other vegetation indices and actual yield.

In summary, the curve statistical yield estimation models show improved accuracy in remote sensing yield estimation for peanuts compared to linear fitting models. The best-fitting single vegetation index curve statistical yield estimation model is the quadratic polynomial yield-NDVI model, with the equation given as $y = 2746.5 - 6357.6x + 3683.6x^2$.

3.3 Construction of Multiple Vegetation Index Yield Estimation Models

3.3.1 Multiple Linear Regression

Based on the correlation analysis between vegetation indices and yield, we can use a combination of multi-temporal and multiple vegetation indices as independent variables to construct a multiple regression model. The fitting results are presented in Table 6.

Table 6. Multiple Linear Regression Model for Peanut Yield Estimation

Development Period Combination	Vegetation Index Combination	R2	RMSE
Mature Period	NDVI-GNDVI	0.58161	0.820
	NDVI-NDRE	0.60231	0.799
	NDVI-LCI	0.60176	0.800
	GNDVI-NDRE	0.50760	0.889
	NDRE-LCI	0.54175	0.858
	NDVI-GNDVI-NDRE	0.63003	0.786
	NDVI-GNDVI-LCI	0.61678	0.793
	NDVI-NDRE-LCI	0.60377	0.803
	GNDVI-NDRE-LCI	0.54640	0.859
	NDVI-GNDVI-NDRE-LCI	0.63064	0.782
Mature Period with Pod-Setting Period	NDVI-GNDVI	0.58902	0.797
	NDVI-NDRE	0.61562	0.771
	NDVI-LCI	0.61983	0.767
	GNDVI-NDRE	0.53057	0.852
	NDRE-LCI	0.54733	0.837
	NDVI-GNDVI-NDRE	0.63673	0.750
	NDVI-GNDVI-LCI	0.63693	0.749
	NDVI-NDRE-LCI	0.62137	0.765
	GNDVI-NDRE-LCI	0.56622	0.819
	NDVI-GNDVI-NDRE-LCI	0.63744	0.749
All Period	NDVI-GNDVI	0.60045	0.786
	NDVI-NDRE	0.61767	0.769
	NDVI-LCI	0.62040	0.766
	GNDVI-NDRE	0.53854	0.845
	NDRE-LCI	0.55099	0.833
	NDVI-GNDVI-NDRE	0.65220	0.733
	NDVI-GNDVI-LCI	0.65349	0.732
	NDVI-NDRE-LCI	0.62369	0.763
	GNDVI-NDRE-LCI	0.59265	0.794
	NDVI-GNDVI-NDRE-LCI	0.65482	0.731

From Table 6, a significant pattern emerges: for each time period, the more indices included in the vegetation index combinations, the better the R² of the yield estimation model. Additionally, for the same combination of vegetation indices, the more peanut development stages utilized, the better the R² of the yield estimation model. Therefore, the yield estimation

model using four vegetation indices across all periods is the model that performs best in the multiple linear regression. The average R^2 values for the fitting models using the same number of vegetation indices in each period are represented in the line graph shown in Figure 5.

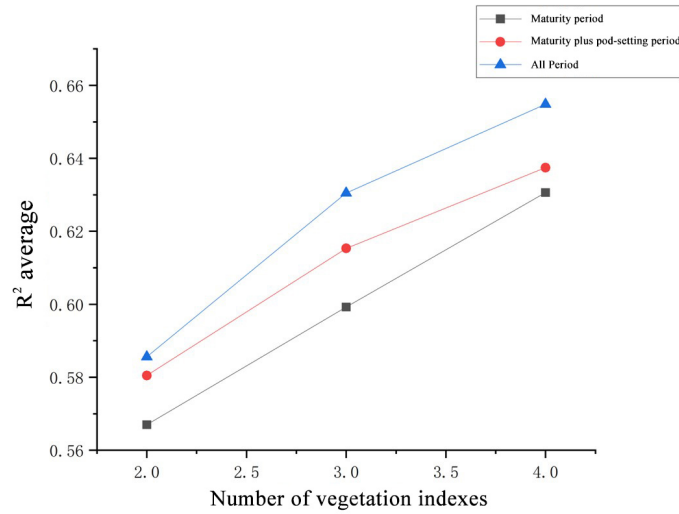


Figure 5. Change of Average R^2 Value

The fitting results obtained by inputting the four groups of vegetation indices as independent variables for the maturity stage, the maturity stage combined with the pod-setting stage, and all three periods are shown in Figure 6.

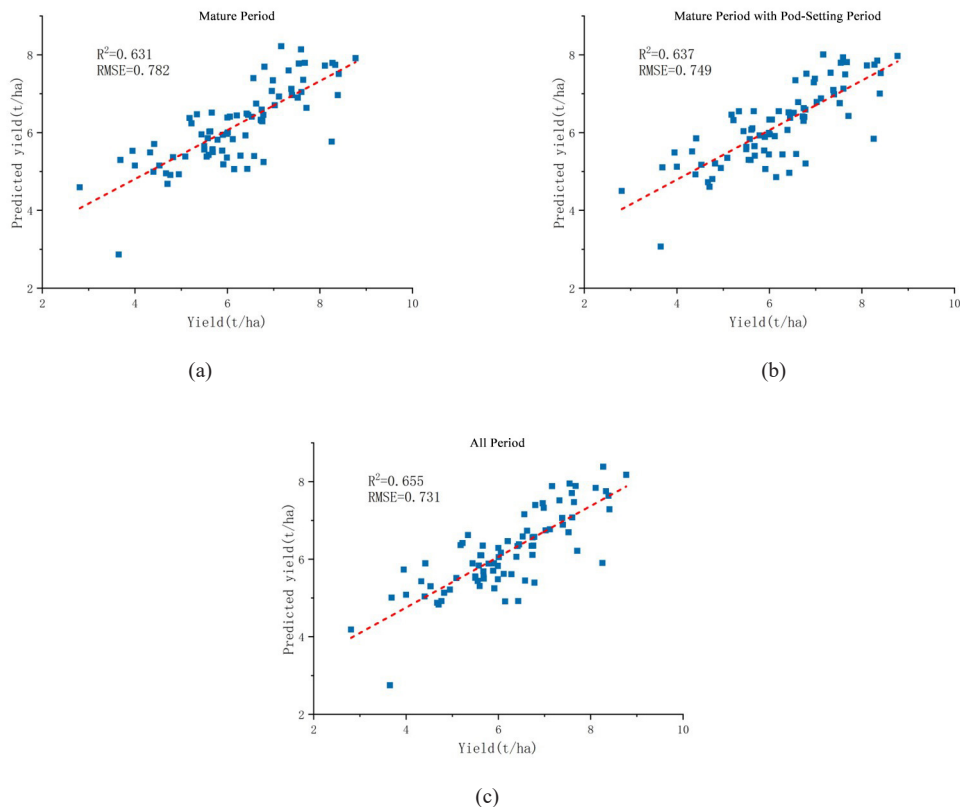


Figure 6. Scatter Plot of Multiple Linear Fitting for the Mature Period, Mature period with Pod-Setting Period, and All Period

(a) Mature Period; (b) Mature Period with Pod-Setting Period; (c) All Period

Based on the analysis above, the four vegetation index combination model across all periods has the best fitting

performance among all combinations, with an R^2 of 0.65482 and an RMSE of 0.731. The multiple linear regression equation is given as: $y = -136.66691 - 14.09848x_1 + 24.9841x_2 + 6.48233x_3 - 13.91531x_4 + 40.57402x_5 + 12.93685x_6 + 26.16262x_7 + 2.56161x_8 + 160.41752x_9 - 73.28624x_{10} + 68.15114x_{11} - 14.45965x_{12}$

3.3.2 Machine Learning

The machine learning models used in this study include Support Vector Machine (SVM), Decision Tree (DT), Random Forest (RF), Extra Trees Classifier (ETR), AdaBoost, Extreme Gradient Boosting (XGBoost), and Multi-Layer Perceptron Neural Network (MLP). Additionally, a Simulated Annealing (SA) algorithm was employed for hyperparameter optimization. The optimal hyperparameters for each machine learning model are presented in Table 7.

Table 7. List of Machine Learning Models and Their Hyperparameters Used in This Study.

Machine Learning Model	Optimal Hyperparameters
Vector Machine	C: 273.4406, Kernel: rbf, Gamma: 0.2814
Decision Tree	Max Depth: 18, Min Samples Split: 9, Min Samples Leaf: 5 Max Features: 11, Max Leaf Nodes: 17
Random Forest	n_estimators: 98, Max Depth: 7, Min Samples Split: 14 Min Samples Leaf: 7, Max Features: 6
Extra Trees Classifier	n_estimators: 192, Bootstrap: False, Criterion: absolute_error Max Depth: 18, Min Samples Split: 14, Min Samples Leaf: 1 Max Features: 6
AdaBoost	n_estimators: 34, Learning Rate: 0.8794
XGBoost	colsample_bytree: 1.0, gamma: 0.2, learning_rate: 0.2, max_depth: 5, min_child_weight: 1, n_estimators: 100, reg_alpha: 0.1, reg_lambda: 0.1, subsample: 0.8
Neural Network	Activation: tanh, Alpha: 0.2668 Hidden Layer Size: (363, 194), Learning Rate: 0.0848 Solver: lbfgs

3.4 Yield Estimation Model Validation

The validation set consisted of 13 samples, which were used to validate the optimal linear fitting and curve fitting models for the single vegetation index, as well as the optimal fitting model from multiple linear regression using multiple vegetation indices and the seven machine learning models. The results are shown in Table 8.

From Table 8, it can be observed that the prediction models utilizing multiple vegetation indices significantly outperform those using single vegetation indices. Among the multiple vegetation index models, some machine learning-based yield estimation models show a remarkable increase in the coefficient of determination. Additionally, the prediction accuracy of the nonlinear models is superior to that of the linear models. For the single vegetation index models, the curve statistical model has an R^2 that is 0.014 higher than that of the linear fitting model. In the multiple vegetation index models, the R^2 of machine learning models is up to 0.149 higher than that of the multiple linear regression model. This indicates that both multiple indices and nonlinearity are two significant advantages in prediction.

Table 8. Performance of the Yield Estimation Model on the Validation Set.

Yield Estimation Model	R^2	RMSE
Linear Fitting	0.627	0.710
Curve Statistics	0.641	0.742
Multiple Linear Regression	0.712	0.425
Support Vector Machine	0.816	0.373
Decision Tree	0.723	0.489
Random Forest	0.640	0.500
Extra Trees Classifier	0.861	0.360
AdaBoost	0.679	0.421
XGBoost	0.718	0.430
Neural Network	0.758	0.435

In this study, the best prediction model is the machine learning model based on the Extra Trees Classifier algorithm, with a coefficient of determination (R^2) of 0.861 and an RMSE of 0.360.

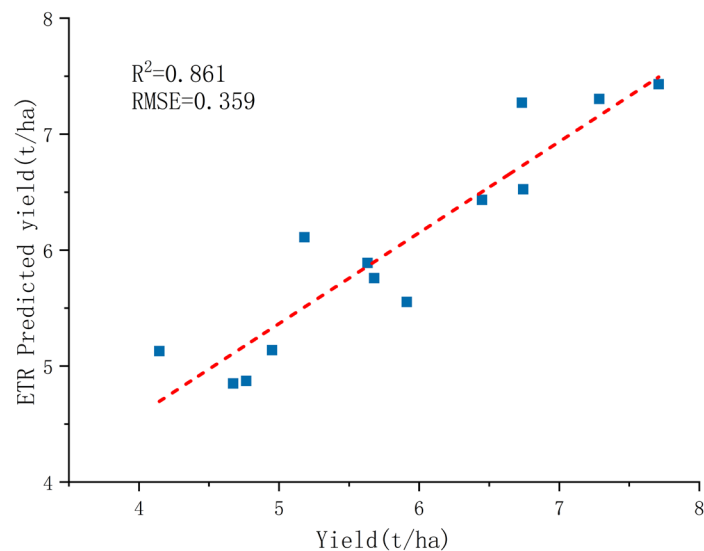


Figure 7. Prediction Scatter Plot of the Extra Trees Classifier Model

4. Discussion

Currently, multispectral remote sensing yield estimation technology has become quite mature for crops such as rice and wheat, but there have been few reports on yield estimation for peanuts. This study attempts to estimate the yield of peanuts, a subterranean crop, using UAV-based multispectral remote sensing. We selected peanut fields in Yanji County, Henan Province, and conducted three flights from July to September 2024 to obtain multispectral remote sensing images of the peanut fields across different time periods. After processing the remote sensing images, we obtained remote sensing data and performed band operations based on vegetation index formulas to derive vegetation index data. Using vegetation index data as independent variables and actual yield as the dependent variable, we constructed and validated yield estimation models using linear regression, curve fitting, multiple linear regression, and machine learning methods. By comparing the performance of each model on the validation set, we identified the optimal yield estimation model. In this study, the best prediction model is the machine learning model based on the Extra Trees Classifier algorithm, with a coefficient of determination (R^2) of 0.861 and an RMSE of 0.360. This method provides a relatively accurate approach for estimating peanut yield based on UAV multispectral remote sensing, enabling real-time and rapid monitoring of peanut production in the study area. It lays a solid foundation for building an economical, applicable, and efficient peanut yield estimation system and serves as a reference for decision-making management in precision agriculture.

References

- [1] Zhou Shudong, Lin Ziqian. Analysis on the Factors Affecting China Peanut Export Based on CMS Model [J]. World Economic and Political Forum, 2013,(05):161-172.
- [2] Wheeler T.,Braun J.-von.Climate Change Impacts on Global Food Security[J]. Science(6145):508-513.
- [3] Yu N, Li L J, Schmitza N, et al. Development of methods to improve soybean yield estimation and predict plant maturity with an unmanned aerial vehicle based platform[J]. Remote Sensing of Environment, 2016, 187(15): 91-101.
- [4] Berni J.,Zarco-tejada P.J.,Suarez L,et al.Thermal and Narrowband Multispectral Remote Sensing for Vegetation Monitoring From an Unmanned Aerial Vehicle[J].IEEE Transactions on Geoscience&Remote Sensing,2009,47(3):722-738.
- [5] Zhang Chunhua,Kovacs John-M.The application of small unmanned aerial systems for precision agriculture:a review[J].Precision Agriculture2012,13(6):693-712.
- [6] Everaerts Jurgen.Remote Sensing and Spatial Information Sciences[J]:CRC Press,2008:117-124.
- [7] Li B, Liu R Y, Liu S H, et al. Monitoring vegetation coverage variation of winter wheat by low-altitude UAV remote sensing system[J]. Transactions of the Chinese Society of Agricultural Engineering, 2012, 28(13): 6.
- [8] Zhang Z J, Li A N, Bian J H, et al. Estimating aboveground biomass of grassland in Zoige by visible vegetation index

- derived from unmanned aerial vehicle image[J]. *Remote Sensing Technology and Application*, 2016, 31(1): 51-62.
- [9] Tian Z K, Fu Y Y, Liu S H, et al. Rapid crops classification based on UAV low-altitude remote sensing[J]. *Transactions of the Chinese Society of Agricultural Engineering*, 2013(7): 109-116.
- [10] Zhou M W, Liu Q H, Liu Q, et al. A method for classification by fusing full-waveform airborne laser scanning data and aerial images[J]. *Remote Sensing Technology and Application*, 2010, 25(6): 821-827.
- [11] Wang S, Guo Z X, Liang X Y, et al. Study on yield estimation model of tobacco vegetation index based on UAV multi-spectral remote sensing data[J]. *Shanxi Agricultural Sciences*, 2021, 49(2): 195-203
- [12] Luo M S, Jing Y S, Xiong S W. A prediction model of rice meteorological yield based on neural networks optimized by genetic algorithm[J]. *Journal of Meteorological Science*, 2012, 32(6): 665-670.
- [13] Bolton Douglas-K., Friedl Mark-A. Forecasting crop yield using remotely sensed vegetation indices and crop phenology metrics[J]. *Agricultural & Forest Meteorology* 2013, 173: 74-84.
- [14] Son Nguyen-Thanh, Chen Chi-Farn, Chen Cheng-Ru, et al. A Phenology-Based Classification of Time-Series MODIS Data for Rice Crop Monitoring in Mekong Delta, Vietnam[J]. *Remote Sensing*, 2013, 6(1): 135-156.
- [15] Han W T, Peng X S, Zhang L Y, et al. Summer maize yield estimation based on vegetation index derived from multi-temporal UAV remote sensing[J]. *Transactions of the Chinese Society of Agricultural Machinery*, 2020, 51(1): 148-155.
- [16] Guan Y Y, Wei Z Y, Wang Y F, et al. Effects of humic acid on maize yield, nitrogen use efficiency and soil properties[J]. *Journal of Henan Institute of Science and Technology (Natural Science Edition)*, 2022, 50(3): 7-15.